IEEE Access
Multidisciplinary | Rapid Review | Open Access Journal

Received September 20, 2016, accepted October 10, 2016, date of publication November 21, 2016,
date of current version January 4, 2017.

Digital Object Identifier 10.1109/ACCESS.2016.2631222

Position-Aided mm-Wave Beam Training Under NLOS Conditions

JUAN C. AVILES[1,2], (Member, IEEE) AND AMMAR KOUKI[1], (Senior Member, IEEE)
[1]Faculty of Electrical and Computer Engineering, Escuela Superior Politécnica del Litoral, Km 30.5 Via Perimetral, P.O.Box. 09-01-5863, Guayaquil, Ecuador
[2]Electrical Department, École de technology supérieure, 1100, rue Notre-Dame Ouest, Montréal (Québec) H3C 1K3, Canada

Corresponding author: J. C. Aviles (javiles@espol.edu.ec)

This work was supported in part by the Escuela Superior Politécnica del Litoral, Guayaquil, Ecuador, and in part by the École de technologie supérieure, Montreal, Canada.

ABSTRACT Ray tracing simulation results indicate that a high-resolution database is not needed to exploit user position knowledge in the 28-GHz band, even in the case of inexact information. A proposed antenna alignment algorithm (using maximum position errors and database resolutions of 10 and 4 m, respectively) that takes advantage of the propagation characteristics knowledge of database points located around the reported location is applied. The results show that the distance between the points can be increased up to 2 m with no considerable negative impact on performance. Simulations also indicate that this outcome is sustained when the maximum power level received at the user equipment varies. The algorithm provides the benefit of a higher initial power delivery and fewer steps, as long as the exact geographical position of the user is within the circular area containing the considered database points. The performance is similar to or better than that of a modified classical hierarchical procedure.

INDEX TERMS Base station (BS), database (DB), non-line of sight (NLOS), millimeter wave (mmW), ray tracing (RT), signal-to-noise ratio (SNR), user equipment (UE).

I. INTRODUCTION

Interest in millimeter-wave (mmW) bands has increased rapidly for applications in cellular systems. Specifically, the 28-38 GHz band is currently the subject of considerable research as a potential candidate to provide 5th-generation (5G) cellular services within a 200 m range [1]. Field measurement data under non-line-of-sight (NLOS) conditions indicate the existence of many propagation paths for a base station (BS)-user equipment (UE) communication link; however, those paths must be ''discovered'' using directional antennas at both the BS and UE. The small wavelength at this frequency band allows many antenna elements to be packed and their radiation patterns to be combined using beamforming techniques to address the large propagation path losses. Nevertheless, that beamforming gain cannot be easily exploited because the discovery process is complex, particularly in systems that use one RF front per side. The one-look limitation of analog beamforming forces both the BS and UE to steer their antenna beams in different directions to establish the antenna lock-on.

A direct application under such a scheme constitutes the classical hierarchical antenna alignment method [2]–[5], in which an initial coarse search procedure that covers a large space is followed by a refined search using smaller-beamwidth antennas. This beam alignment method, which is typically exploited in the 60 GHz band, must be redesigned for use at 28 GHz because the application of low-gain antennas (i.e., omnidirectional), whether in transmit or receive beamforming mode, limits the possibility of obtaining UE feedback, even with narrowband signals. This effect could generate a mismatch between the discoverable and actual supportable RF coverage [6].

Many alternatives have already been proposed. The standard compressed channel-sensing techniques that leverage the sparsity property of mmW channels can provide an accurate representation of the power angle profile (PAP) and considerably reduced beamforming overhead [7]; nevertheless they are sensitive to additive noise [8]. This effect may primarily have an impact in NLOS locations, where the signal-to-noise ratio (SNR) may not be sufficiently high. In contrast, as a substitute for the versatility that can be obtained from the costly digital beamforming mode, recent research has considered the use of the so-called hybrid beamforming combined with adaptive compressed sensing to estimate the channel. This technique requires the

application of more than one RF chain at both the BS and UE sides [9], [10].

One approach not yet fully explored utilizes the site-specific propagation characteristics in which the system is deployed. This knowledge can be exploited at the BS in the form of a database (DB) linked to the position of the UE [11]. Location information is becoming more readily available as a built-in feature (i.e., Global Positioning System (GPS) or network positioning system) with an increasing degree of accuracy. In fact, some researchers share the vision that context and location information can address some of the key challenges in 5G networks [12]. The application of a DB has the potential to allow for a faster connection in terms of the number of steps and an initial larger antenna gain for the benefit of the antenna alignment.

Previous studies in this direction include a proposal to exploit the geographical position of the UE (assumed to be acquired through a separate control plane operating at microwave frequency in legacy infrastructure) to improve a cell search procedure. Two search algorithms are introduced in [13] and [14] that use a starting beamwidth and azimuth angle related to the position of the UE. The initial version of an enhanced discovery procedure [13] is improved via a learning approach [14] that uses past successful connections saved in a fingerprint map. In [15], a 3-D ray tracing model is applied as a propagation-prediction engine to evaluate the performance of three cases of beamforming in an indoor communication system. The ray tracing itself is proposed as a real-time prediction tool to assist future beamforming techniques. In [13]–[15] the BS and UE are equipped with directional and omnidirectional antennas, respectively. In [16], it is argued that analog beamforming can still be a viable choice when context information regarding the mmWave base stations is available at the mobile station. However, these studies do not consider the effect of a directional antenna or its rotation at the UE side, both of which are key factors for the initial network access [17] or the alignment process.

In this work, we study the application of specific propagation knowledge at 28 GHz in the form of a DB linked to the geographical position of the UE. 3D ray tracing simulations in two different areas inside an urban environment are performed for the cases in which the BS knows the exact and inexact location of the user. We propose an algorithm that applies a hierarchical-like alignment scheme and utilizes the observation that the BS angles linked to the first propagation path repeat exactly or approximately at other close geographical points around an arbitrary UE position. Our previous work [18] facilitated the application of a reduced DB.

Through simulations, the proposed algorithm is found to have a performance that is similar to or better than (in terms of received power) that of a modified classical hierarchical beam alignment procedure. This result is accomplished as long as the exact position of the user is within a circular area containing the group of neighbor DB points considered. The algorithm facilitates the application of a narrow-beamwidth antenna at the BS in the initial stage of the antenna alignment process. Thus, it provides the advantage of an increased starting power delivery and of a reduced total number of steps, even in the case of inexact location information.

In addition, the effects of the DB resolution, maximum position error and radius of the circular area for static and variable conditions are analyzed.

We use the following notation: $\boldsymbol{A}$ is a matrix, $\|\boldsymbol{A}\|_p$ is the p-norm of $\boldsymbol{A}$, $\boldsymbol{v} = \boldsymbol{A}(:, i)$ is a vector, $\boldsymbol{w} = [\boldsymbol{v_1}; \boldsymbol{v_2}]$ is the vector obtained after stacking the vectors $\boldsymbol{v_1}$ and $\boldsymbol{v_2}$, $[\theta_1{:}\Delta\theta{:}\theta_2]$ is the set of values $(\theta_1, \theta_1 + \Delta\theta, \theta_1 + 2\Delta\theta, \ldots, \theta_2)$, card(.) is the cardinality of a set, and unique(.) is a computation operator that eliminates the repetition of an element in a defined group of angles.

The remainder of the paper is organized as follows. Section II describes the system model and simulation methodology. A description of the proposed algorithm is provided in Section III. In Section IV, we consider the performance of the algorithm under static conditions and variations in the power received at the UE located in fixed positions. Finally, concluding remarks are provided in Section V.

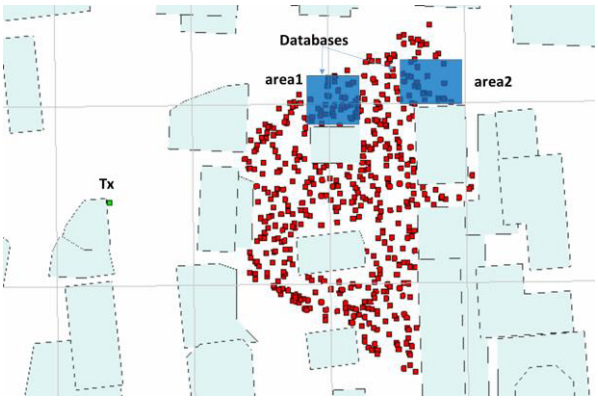

FIGURE 1. Simplified cellular system.

II. SYSTEM MODEL AND SIMULATION METHODOLOGY

A. SYSTEM MODEL

Consider a one sector time division duplex (TDD) cellular system (Figure 1) with dimensions of 60° × 200 m operating in a specific urban environment, where the predominant RF propagation corresponds to a street canyon type. The system is composed of one BS and many UEs randomly located at NLOS positions within the service area. All devices are equipped with horn antennas.

The BS knows the geographical position of the UE with a certain error relative to its exact location. The position information is assumed to be periodically reported to the BS using a separate control layer operating on a lower microwave band. The BS has a DB with propagation information of 2,652 and 2,944 points uniformly distributed in two areas $\hat{a}_1$ (25 m × 25 m) and $\hat{a}_2$ (23 m × 32 m), respectively, (blue squares in Figure 1). The DB points are separated by 0.5 m (database

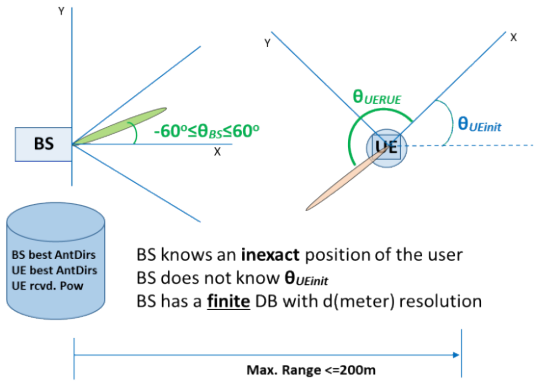

FIGURE 2. BS with a database. The UE has a random initial angle.

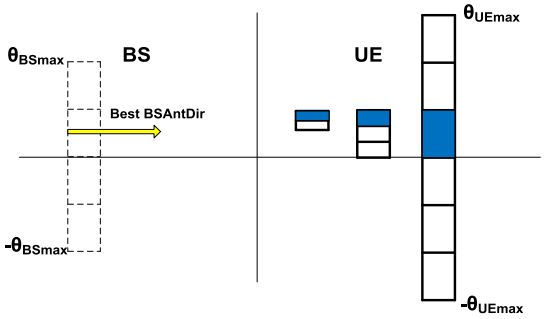

FIGURE 3. The BS applies a high antenna gain in the initial stage of the alignment procedure.

resolution DB_{res}). $\hat{a}_1$ corresponds to an area with a higher SNR than $\hat{a}_2$.

There are 44 and 100 arbitrary positions within the limits of $\hat{a}_1$ and $\hat{a}_2$, respectively, at which the UE can be located. The UE antenna beam is assumed to have a random initial angle θ_{UEinit} (physical azimuth rotation) in the range [0°:5°:355°]. This angle is kept fixed for the entire block of measurements from which it starts to measure the power levels in consecutive fixed angle steps (Figure 2). At the end of that block, the UE feeds back the best BS angle. The UE angle is referred as θ_{UERUE}.

B. SIMULATION METHODOLOGY

An accurate 3D commercial ray tracing tool (Wireless Insite) [19] is applied to simulate the wireless channel for a fixed transmitter BS and many receivers. The BS power is set to 30 dBm, and the center frequency is set to 28 GHz. A combination of 10° (24.5 dB gain) and 30° (15 dB gain) pyramidal horn antennas [20], all with vertical polarization, together with a narrow band signal of 1 MHz is considered. Such scheme becomes necessary to ensure (Appendix) a fair comparison between the proposed and a referential procedure. Phased antenna arrays[1] [21] can be used instead.

Propagation data (received power, angle of departure, and angle of arrival of the multipath components) applying all BS-UE angle combinations are generated for each of the UE positions and DB points. The angles are assumed to vary in azimuth only. A distance of 0.5 m between contiguous DB points facilitates subsequent simulations with lower resolutions (e.g., 1 m, 1.5 m, and 2 m). The following BS discrete angle sets are considered: the best ones (49) in the range [−60°:1°:60°] obtained from [18], [−55°:10°:55°] and [−57.5°:5°:57.5°] using a 10° horn antenna and [−45°:30°:45°] with a 30° horn antenna. The UE discrete angles applied are [0°:5°:355°] with both 10° and 30° horn antennas and [2.5°:5°:357.5°] with a 10° horn antenna only. The 5° angle step at the UE side is chosen as a compromise between resolution and computation time.

The BS antenna height is set to 8 m, whereas the UE antenna height is fixed at 1.5 m. The BS and UE use only one RF front each. The general settings for the tool (full 3D) are 6 reflections, 1 diffraction, 0.1° ray spacing, and uniform material[2] for all the building walls. The area under study corresponds to a small city in Rosslyn, Virginia, USA (Figure 1), where the exterior buildings walls are assumed to be made of brick. The BS is installed in front of three buildings with heights of 14 m, 38 m (center), and 6 m located across the street at a distance of approximately 48 m. The UE and DB points are located along the streets, primarily behind the two taller buildings (14 m and 38 m high). As a result, NLOS propagation conditions exist at all positions.

III. PROPOSED HIERARCHICAL METHOD

To improve the initial BS-UE connection in the 28 GHz band using only one RF front, we propose an alternate version of a hierarchical alignment method that leverages the approximate user position knowledge. In this procedure, the BS initially selects a small set of angles to directly illuminate the intended UE using a high-gain antenna (Figure 3).

Given that θ_{UEinit} cannot be predicted from the saved DB information, the UE determines the best BS and UE angles using a sequence of power measurements. The UE seeks the highest received power level by steering its antenna with a defined beamwidth. After a round of power measurements and data feedback, the UE changes the beamwidth of its antenna to one with a higher gain. This method has the advantages of faster alignment of the BS-UE main beams and a higher starting received power level. For comparison

[1]The application of a horn antenna (instead of a 2-D array) simplifies the simulations because it excludes the beamwidth variation with beam steering and facilitates the identification of the UE angle in a 360 degree range.

[2]The adoption of a uniform building setup and material characteristics in the ray tracing tool generates results that are an approximation to reality. The application of non-uniform parameters requires a detailed description of the environment. For this reason it is not claimed an absolute gain value in the benefit of exploiting the propagation characteristics knowledge of the site but only a relative gain. This latter resulting in the comparison between the proposed and a referential method, both under the same site conditions.

purposes, we contrast the proposed method to a modified classical hierarchical procedure.[3]

A. BS KNOWS THE EXACT UE POSITION X_{EP} AND HAS DATABASE INFORMATION FOR THAT POSITION

The BS (equipped with a 10° horn antenna) illuminates the UE with the best BS angle extracted from the DB. In contrast, the UE samples the received power in equal angle steps; it initially uses a 30° horn antenna and then switches to a narrower one (10°). The best UE angle cannot be applied directly from the DB information because of θ_{UEinit}, which is unknown to the BS. The proposed Algorithm 1 is as follows:

1) The BS (10° horn antenna) applies the best θ^b_{BS} obtained from the DB based on the exact position reported by the user.
2) The UE (30° horn antenna) measures the power levels $\boldsymbol{v} = [p_1, p_2, .., p_{12}]^T$ at $\theta_{UERUE} = \frac{(n-1)\pi}{6}$; n = 1, 2, .., 12.
3) The UE generates:

$$[\boldsymbol{v}_{ext}]_{24x1} = [\boldsymbol{v}\,(7{:}12,\,1)\,;\,\boldsymbol{v}\,(1{:}12,\,1)\,;\,\boldsymbol{v}(1{:}6,\,1)]$$

4) The UE applies interpolation and curve fitting to $[\boldsymbol{v}_{ext}]_{24x1}$ to obtain $[\boldsymbol{v}''_{ext}]_{720x1}$; and then calculates:

$$[\boldsymbol{v}'_{\text{ext}}]_{360x1} = \boldsymbol{v}''_{ext}(181{:}540,\,1).$$

5) The UE determines the angle where the maximum power is received:

$$\theta^{1^\circ}_{UEmaxPowRUE} = \underset{\theta_{lUE}}{\text{argmax}}\left(\boldsymbol{v}'_{\text{ext}}\right); \quad l = 1, 2, \ldots, 360$$

6) The UE maps $\theta^{1^\circ}_{UEmaxPowRUE} \in [0°{:}1°{:}360°)$ to $\theta^{5^\circ}_{UEmaxPowRUE} \in [0°{:}5°{:}360°)$.
7) The UE decreases the beamwidth of its antenna to 10° and then finds its final best angle θ^b_{UERUE} by applying a refinement stage of power measurements at $\theta^{5^\circ}_{UEmaxPowRUE} + (\pm 5°, \pm 10°)$.

The 12 power values of $\boldsymbol{v}$ corresponding to angles $[\theta_{UEinit} + 0°{:}30°{:}\theta_{UEinit} + 330°]$ are arranged as an extended vector $[\boldsymbol{v_{ext}}]_{24x1}$ to follow the 'circular' characteristic of the PAP around the limits $\theta_{UEinit}+0°$ and $\theta_{UEinit}+330°$. An interpolation and curve-fitting procedure is applied to $[\boldsymbol{v_{ext}}]_{24x1}$ to obtain $\left[\boldsymbol{v}''_{ext}\right]_{720x1}$ and then $\left[\boldsymbol{v}'_{ext}\right]_{360x1}$; this latter containing power levels associated with the angles [0°:1°: 360°). Such procedure (which changes the angle resolution from 30° to 1°) helps avoid the inconvenience of the highest-power sample level not always coinciding with the maximum possible value. That deviation generates an UE angle determination error in the range [−15°:5°:15°]. The interpolation method may fail to provide an appropriate estimate of $\theta^{1^\circ}_{UEmaxPowRUE}$ when there are two power lobes very close to each other, producing a considerably wider PAP. Such scenario does not appear frequently. The UE maps its angle $\theta^{1^\circ}_{UEmaxPowRUE}$ to $\theta^{5^\circ}_{UEmaxPowRUE}$ in the refinement stage. Figure 4 shows the power lobes, the PAP of the DB point considered (for $\theta_{BS} = -57°$) and the sample power values read by the UE using a 30° beamwidth antenna.

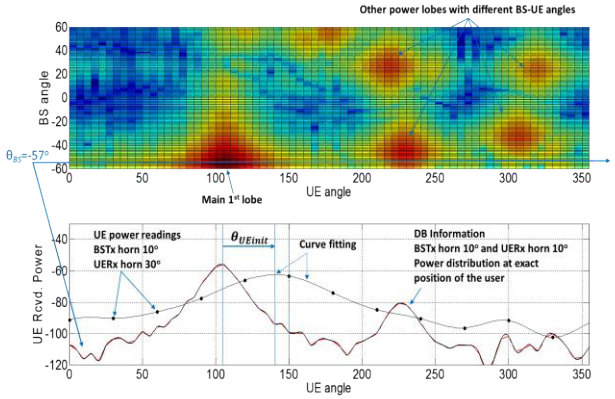

FIGURE 4. DB reference curve and UE power readings.

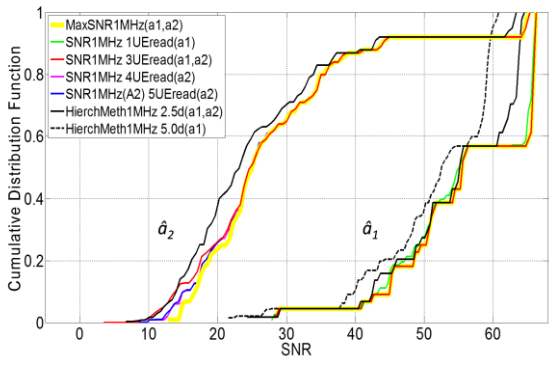

FIGURE 5. Performance of algorithm 1 versus a modified classical hierarchical method in $\hat{a}_1$ and $\hat{a}_2$.

Figure 5 shows the performance of Algorithm 1 (red curve for area 1 ($\hat{a}_1$) and the blue curve for area 2 ($\hat{a}_2$)). Algorithm 1 outperforms the modified classical hierarchical method (solid black) in both areas. The power difference received at the UE is mainly caused by a higher power obtained by applying the best angles at the BS (extracted from the DB), in contrast to simply using approximate angles via the modified classical

[3]The BS starts the alignment by steering its 30° beam in the directions of −45°, −15°, 15°, and 45°. For each BS angle, the 30° UE beam is switched sequentially in the range $[\theta_{UEinit}+0°{:}30°{:}\theta_{UEinit}+330°]$. Once the UE reports back the best BS angle $\theta^i_{stage1BS}$, the UE fixes its 30° beam along the corresponding best direction $\theta^j_{stage1UE}$. In the following stage, the BS changes its antenna beamwidth to 10° and then switches in the range $[\theta^i_{stage1BS} - 10°{:}10°{:}\theta^i_{stage1BS} + 10°]$. The UE reports back the best $\theta^i_{stage2BS}$, which is fixed by the BS for the following part. The UE changes its antenna beamwidth to 10° and then switches its angle in the range $[\theta^j_{stage1UE} - 10°{:}10°{:}\theta^j_{stage1UE} + 10°]$ and finds the best $\theta^k_{stage2UE}$. For a fair comparison using antennas with a beamwidth of up to 10°, the UE fixes $\theta^k_{stage2UE}$ and the BS beam is allowed to move $\theta^i_{stage2BS} \pm 2.5°$. The UE feeds back the best BS angle $\theta^l_{stage3BS}$, which is fixed for the next stage. Finally, the UE finds the best angle $\theta^k_{stage3UE}$ from $\theta^k_{stage2UE} \pm 2.5°$. The best combination corresponds to $\theta^l_{stage3BS}, \theta^k_{stage3UE}$. A 2.5° step was applied instead of the correct 5°. The main purpose was to have a more strict reference for the comparison.

hierarchical method. The starting antenna gain difference of 9.5 dB (39.5-30 dB) is important for achieving a better initial RF coverage in the alignment process. The maximum power difference reaches approximately 3 dB in $\hat{a}_1$ and $\hat{a}_2$, but it is generally smaller in $\hat{a}_1$. The plots in $\hat{a}_1$ indicate that the maximum received SNR is approximately the same in many UEs (almost vertical line around 65 dB). Specifically the SNR values vary from 65.35dB to 66.27dB in 41% of the UE positions. Those UE positions receive power with the BS angles 27°, 28°, 29° and 30°. For reference purposes, the dashed black line represents the power obtained in the application of the modified hierarchical method in $\hat{a}_1$ using a 5° step in the final alignment stage instead of 2.5°. The yellow curve represents the maximum possible power at the UE position considering all combinations of the BS and UE angles.

Once the UE determines the angle $\theta^{5°}_{UEmaxPowRUE}$, a refinement of three additional power measurements (solid red line) at the angle offsets [−5° 0° 5°] are necessary for a user located in $\hat{a}_1$ and five (solid blue line) at the angle offsets [−10° −5° 0° 5° 10°] for a user in $\hat{a}_2$. The SNR obtained at $\theta^{5°}_{UEmaxPowRUE}$ in $\hat{a}_1$ (only one reading; green curve) can be lower than that obtained using the modified classical hierarchical method, thus generating the need of a larger number of UE readings. The same situation appears in $\hat{a}_2$, where the performance with only 3 reads is not superior to the reference curve for SNR ≤ 14 dB. A special procedure using 4 UE reads (magenta line) yields similar results as obtained with five reads in $\hat{a}_2$. In the latter procedure, the UE determines the angle of the next power readings based on the tendency of the last two power values.

B. BS KNOWS THE EXACT UE POSITION X_{EP} AND HAS A DB WITH A RESOLUTION (DB_{res}) OF d METERS

Because it is not possible to collect propagation information for all possible UE positions, the BS must rely on a DB with a finite number of points separated by DB_{res} meters. One possibility is to apply Algorithm 1 using the best BS angle for the closest BD point. Figure 6 shows the performance in $\hat{a}_1$ using this criterion for DB_{res} of 1, 1.5, 2, 3 and 4 m. As expected, the received power level at the UE is lower when the resolution of the DB is lower. For this case, given that there are only 44 arbitrary fixed UE positions, we simulate the application of the closest point by selecting DB points located within a distance $r \leq \frac{d}{2}\sqrt{2}$ from the reported (exact) UE location considering that the DB is arbitrarily shifted in x and/or y coordinates relative to that position.

For the specific area $\hat{a}_1$, Figure 6 indicates that the selection of the best BS angle under the criteria of the 'closest point' in DBs with resolution larger than 2 m is not competitive (in terms of power delivered to the UE) against the modified classical hierarchical beam training (solid black curve). However, the selection of the best angle corresponding to one of the four close BD points located in the vertex of the square enclosing the UE improves the performance to levels similar to the maximum power possible. This improvement occurs because the best BS discrete angle for the exact location of the UE is repeated in other nearby points that do not necessarily coincide with the nearest DB point.

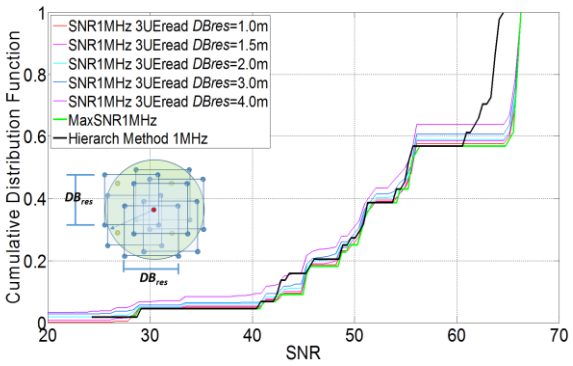

FIGURE 6. SNR obtained using the best BS angle for the DB point closest to the UE (different DB resolutions).

C. BS KNOWS AN INEXACT UE POSITION X_{RP} AND THE DB HAS A DB_{res} OF d METERS

The knowledge of X_{EP} is rather an idealistic situation. A GPS typically has an inherent distance error $e_p = ||X_{RP} - X_{EP}||_2 \leq e_{pmax}$ that complicates an otherwise straightforward application of Algorithm 1 because it introduces an uncertainty regarding the best BS angle to be applied. Taking the information directly from the closest DB point to an incorrect location can produce a large decrease in the received power. A higher DB_{res} is not useful in this scenario.

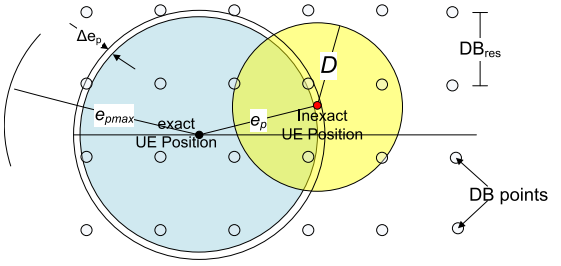

FIGURE 7. Circular area of DB points $å_{DB}$ of radius D around the reported inexact UE position.

A circular area $å_{DB}$ (radius D) containing a group of M-DB points in the neighborhood of X_{RP} is used as an information base in this case (Figure 7).

The geographical distribution of the best discrete BS and UE angles in $\hat{a}_1$ and $\hat{a}_2$ is of interest. These angles repeat themselves at many locations, and there are few different angles serving the DB points around the positions of the UE.

Figure 8 shows a group of 800 DB points (blue) inside $å_{DB}$ in $\hat{a}_1$, and all locations of the UE (black dots) and DB points (various colors) in $\hat{a}_1$ and $\hat{a}_2$ ($DB_{res} = 0.5$ m, $D = 8$m). The different colors represent the best BS and UE angles for the DB points. Figure 9 shows (blue dots) the twelve best angle pairs (θ_{kBS}, θ_{lUE}) serving all DB points in $å_{DB}$ ($\hat{a}_1$). The

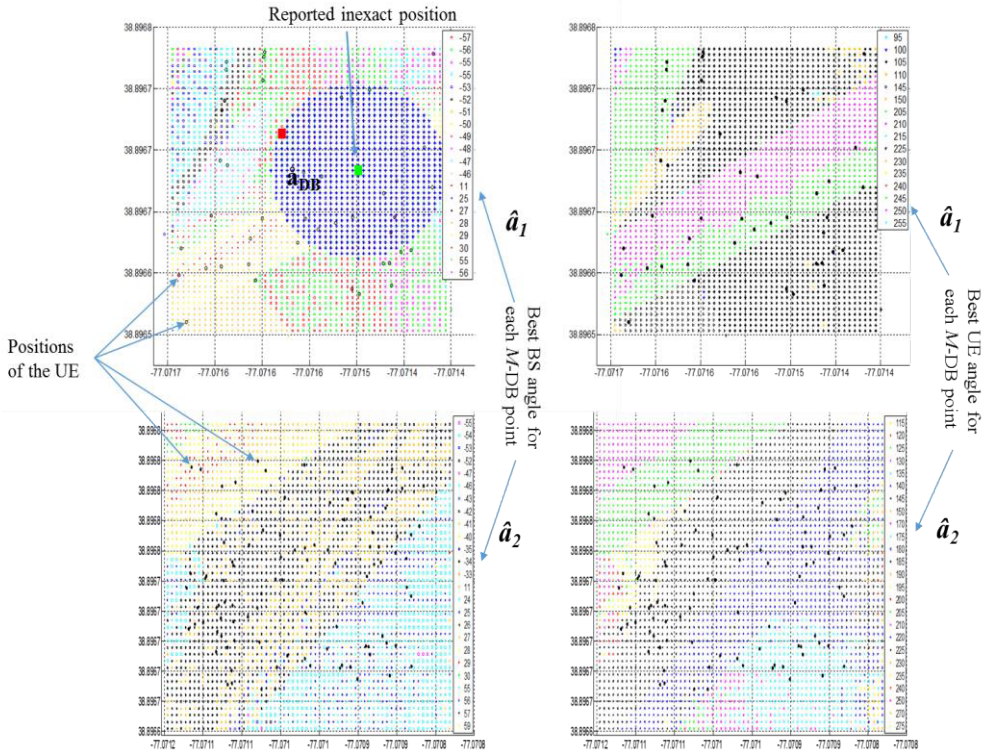

FIGURE 8. *M*-DB points in $\mathring{a}_{DB}$ (blue dots) around the reported inexact position (green square), UE positions (black dots) and geographic distribution of best BS and UE angles in areas $\hat{a}_1$ and $\hat{a}_2$. $DB_{res} = 0.5$ m.

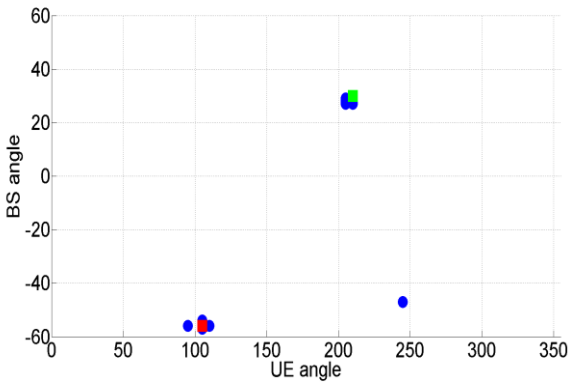

FIGURE 9. ($\hat{a}_1$) Best angles (first power lobe) associated with all *M*-DB points in $\mathring{a}_{DB}$ and the UE (exact and inexact positions).

best angle pair for the UE located at the exact and inexact positions are represented by a small red and green square, respectively.

Given a DB_{res}, there is a trade-off between D and the position error e_p. A greater repetition of the best BS angle within $\mathring{a}_{DB}$ makes its determination easier and relaxes the knowledge requirement of the exact position of the UE. In contrast, a larger D is not necessarily better because it also increases the number of distant DB points that are best served with different BS angles.

To approximate a relationship between D and e_p, we consider two methods as follows:

a) Center $\mathring{a}_{DB}$ at the inexact location X_{RP} reported by the UE and calculate ($p_{rBestBSang}$) the probability that the best BS angle of the UE repeats in the DB points within $\mathring{a}_{DB}$ as D varies. The same DB points are used randomly as candidates for the inexact UE positions. Considering that few DB points are located at the exact error distance e_p from X_{EP} and that it is of interest to obtain adequate statistics, we select the points with position errors e_p in the range [*value*, *value* + Δe_p] ($\Delta e_p = 0.25$) for $DB_{res} = 0.5$ m. Figure 10 and Table 1 indicate that the value of $D = D^{(maxprob)}$ that maximizes $p_{rBestBSang}$ is equal to or larger than e_p; that is, $D^{(maxprob)} \geq e_p$. For $e_p = 0$ (solid yellow), $\mathring{a}_{DB}$ is centered at the exact position of the UE and $p_{rBestBSang}$ decreases monotonically as D increases. Given that e_p is an unknown variable, its use becomes impractical.

b) Apply e_{pmax} as a fixed reference and determine the value of D for which $p_{rBestBSang}$ maximizes under the condition $e_p \leq e_{pmax}$. The parameter e_{pmax} is associated with the accuracy of the positioning system error and is easily available. Figure 10 shows that $p_{rBestBSang}$ (dashed lines) decreases with D, in which case its minimum value $D = e_{pmax}$ must be selected. The decrease of $p_{rBestBSang}$ at $e_p = e_{pmax}$ relative to $e_p < e_{pmax}$ is moderate (4th column in Table 1). Note that the percentages of such variation in the range [0.5, e_{pmax}] become an upper bound because it is likely that $e_p \geq 0.5$ (on average) for larger values of e_{pmax}. Considering both methods, we approximate the radius of $\mathring{a}_{DB}$ as $D \gtrsim e_{pmax}$.

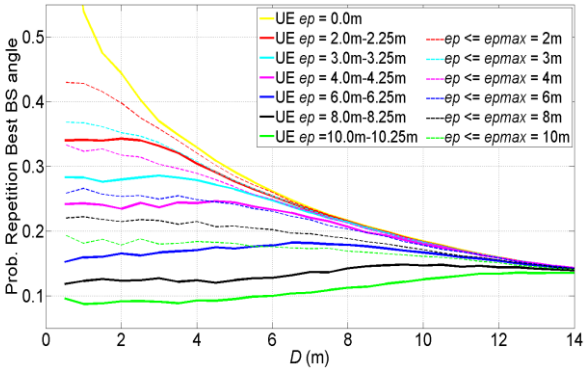

FIGURE 10. Probability of the BS angle repetition versus D in $\mathring{a}_{DB}$ ($\hat{a}_1$) for the condition $e_p \in [value, value + \Delta e_p]$ and $e_p \leq e_{pmax}$. $DB_{res} = 0.5$ m.

TABLE 1. $D^{(maxprob)}$ and the difference in $p_{rBestBSang}$ for $0.5\text{m} \leq e_p \leq e_{pmax}$.

Position Error e_p (m)	D (m) maxProb.	Max. position error e_{pmax}	Difference in $p_{rBestBSang}$ $0.5\text{ m} \leq e_p \leq e_{pmax}$
$2.0 \leq e_p \leq 2.25$	2	$e_p \leq e_{pmax} = 2$	0.0314 (7.3%)
$3.0 \leq e_p \leq 3.25$	3	$e_p \leq e_{pmax} = 3$	0.0320 (8.7%)
$4.0 \leq e_p \leq 4.25$	4.5	$e_p \leq e_{pmax} = 4$	0.0443 (14.0%)
$5.0 \leq e_p \leq 5.25$	5.5	$e_p \leq e_{pmax} = 5$	0.0361(12.3%)
$6.0 \leq e_p \leq 6.25$	6.5	$e_p \leq e_{pmax} = 6$	0.0273(10.5%)
$7.0 \leq e_p \leq 7.25$	8.5	$e_p \leq e_{pmax} = 7$	0.0159(6.9%)
$8.0 \leq e_p \leq 8.25$	9.5	$e_p \leq e_{pmax} = 8$	0.0320(14.5%)
$9.0 \leq e_p \leq 9.25$	11.5	$e_p \leq e_{pmax} = 9$	0.0256(12.9%)
$10.0 \leq e_p \leq 10.25$	12.5	$e_p \leq e_{pmax} = 10$	0.0334(17.2%)

Once the value of D is estimated, the BS determines a small set (G) of angles to illuminate the UE. Our initial simulations indicated that the identification of those angles in G based on the criteria of maximum power at the M-DB points and their probability of repetition in $\mathring{a}_{DB}$ was the best approach. Only 3 angles are sufficient to be competitive relative to the modified classical hierarchical method. The UE finds the definitive best BS and UE angles through a sequence of power level measurements.

Based on these observations, the following algorithm is proposed:

a. Identify all M-DB points located inside a circular area $\mathring{a}_{DB}$ of radius $D \gtrsim e_{pmax}$ centered at X_{RP} such that this area always includes the exact position X_{EP} of the user.

b. Identify the best BS and UE angle pair for each one of the M-DB points ($\boldsymbol{A}'_{Mx2}$) by testing the received power for all combinations of the $\overline{N}$ BS angles obtained from [18] and the set of UE angles $\{0°, 5°, \ldots, 355°\}$.
Given that many of those angles are repeated, the initial M-BS and M-UE angles are reduced in number to N-BS and L-UE angles by selecting only those that are different. Furthermore, because the latter sets can still be large, these are further reduced by the following pre-selection procedure:

- The N-BS angles are ordered according to a sum of power differences. For this effect, the matrix $[\boldsymbol{Q}'']_{MxN}$ and vector $[\boldsymbol{t}]_{Mx1}$ are defined. Specifically, each element of $\boldsymbol{Q}''$ is calculated as: $q''_{i,k} = \boldsymbol{Q}''(i,k) = \max\left[P_{i,\theta_{kBS},0°}, P_{i,\theta_{kBS},5°}, ., P_{i,\theta_{kBS},355°}\right]$, where $P_{i,\theta_{kBS},5°}$ represents the power at DB-point i (DB_{pi}) in which the BS and UE apply the angles θ_{kBS} and 5°, respectively. $q''_{i,k}$ is the maximum power at DB_{pi} considering all the power values measured when the UE antenna beam (10°) is rotated 360° in 5° increments using θ_{kBS} ($i = 1, 2, 3, .., M$ and $k = 1, 2, 3, .., N$).
Similarly, $\boldsymbol{t}$ contains the maximum power possible at each of the M-DB points considering all combinations of the N-BS and 72-UE angles, that is, $\boldsymbol{t}(i,1) = \max\left(\left[q''_{i,1}, q''_{i,2}, \ldots., q''_{i,N}\right]\right)$.
The sum of power differences is $[\mathbf{difpow}]_{1xN}$, where $\text{difpow}_k = \sum_{i=1}^{M} \left|\boldsymbol{t}(i,1) - \boldsymbol{Q}''(i,k)\right|$.
The BS sorts (ascend) the values of $\mathbf{difpow}_{mw}$ and orders the N-BS angles based on that sorting index.
- Starting from the first angle in the ordered set and considering that the BS antenna has a beamwidth '*bwdth*', we discard angles within the range $\theta_{jBS} \pm \left(\frac{bwdth}{2}\right)$, except θ_{jBS}. This proposal is reasonable because the difference in power delivered by the BS using the eliminated angles relative to that of the closest θ_{kBS} would vary approximately up to 1.5 dB and the largest number of well separated BS angles must be explored. The BS angles left are used directly in the illumination of the UE if the number (n_a) of them was less than or equal to three (set G). In case of $n_a > 3$, the remaining BS angles are ordered based on their percentage of repetition inside $\mathring{a}_{DB}$. Only the three most probable angles are considered to illuminate the UE (set G).

c. Using a 30° horn antenna, the UE measures the power (for each BS angle in the set G) at $\theta_{UERUE} = (n-1)\pi/6$; $n = 1, 2, \ldots, 12$. The data sets are saved as $\boldsymbol{v}_1$, $\boldsymbol{v}_2$ and $\boldsymbol{v}_3$.

d. UE applies interpolation and curve fitting to each group of power measurements (as in Algorithm 1). This procedure provides 360 power values (corresponding to 360 degrees) for each BS angle. The best BS and approximate best UE angles are determined by comparing the power levels at the UE.

e. The UE feedbacks the best BS angle θ^b_{BS}.

f. The BS illuminates the UE using θ^b_{BS}.

g. Using a higher-gain antenna (10°), the UE determines its final best angle by applying a refinement stage of power measurements at the angle offsets $[-10°, -5°, 0°, 5°, 10°]$.

The proposed Algorithm 2 is detailed as follows:

1. The BS identifies all *M-DB* points with coordinates X_i that satisfy: $H = \{X_i / ||X_{RP} - X_i||_2 \leq D\}$; $D \gtrsim e_{pmax}$; $i = 1, 2, \ldots, M$;

2. The BS obtains $\boldsymbol{A}'_{Mx2}$ from the DB, where

$$\boldsymbol{A}'(i,1:2) = \left\{ (\theta'_{i,vBS}, \theta'_{i,wUE}) / \underset{\substack{j=1,2,3,...,\bar{N} \\ l=1,2,3,...,72}}{\operatorname{argmax}} \left(P_{i,\theta_{jBS},\theta_{lUE}}\right) \right\};$$

$\theta'_{i,vBS} \in \{\theta_{1BS}, \theta_{2BS}, .., \theta_{\overline{N}BS}\}$;

$\theta'_{i,wUE} \in \{0°, 5°, 10, \ldots, 355°\}$;

$P_{i,\theta_{jBS},\theta_{lUE}}$ = Power at DB_{pi} using the angle pair $(\theta_{jBS}, \theta_{lUE})$.

3. The BS determines:

$$\left[\boldsymbol{a}_{\theta_{BS}}\right]_{Nx1} = \text{unique}(\boldsymbol{A}'(:,1));$$
$$\left[\boldsymbol{a}_{\theta_{UE}}\right]_{Lx1} = \text{unique}(\boldsymbol{A}'(:,2)); \quad N \leqslant M;\ L \leqslant M$$

4. The BS constructs:
   - $\left[\boldsymbol{Q}''\right]_{MxN}$, where each element $q''_{i,k}$ is given by:

$$q''_{i,k} = \max\left[P_{i,\theta_{kBS},0°}, P_{i,\theta_{kBS},5°}, ., P_{i,\theta_{kBS},355°}\right];$$
$$\theta_{kBS} = \boldsymbol{a}_{\theta_{BS}}(k,1); \quad k = 1,2,..,N.$$

   - $[\boldsymbol{t}]_{Mx1}$; where $t_i = \max\left(\boldsymbol{Q}''(i,1:N)\right)$.
   - $[\mathbf{difpow}]_{1xN}$, where $\text{difpow}_k = \left\|\boldsymbol{t} - \boldsymbol{Q}''(:,k)\right\|_1$.

5. The BS orders the angles in $\boldsymbol{a}_{\theta_{BS}}$

$$\text{Indx} = \underset{ascend}{\text{sort}}\,[\mathbf{difpow}]; \quad \boldsymbol{a}^{ord}_{\theta_{BS}} = \boldsymbol{a}_{\theta_{BS}}(\text{Indx},1)$$

6. The BS generates $\boldsymbol{b}_{\theta_{BS}} = \left[a^{ord}_{\theta_{BS}}(1,1), a^{ord}_{\theta_{BS}}(y,1), \ldots\right]^T$ by discarding angles in the range $\boldsymbol{a}^{ord}_{\theta_{BS}}(j,1) \pm \left(\frac{bwdth}{2}\right)$, except $\boldsymbol{a}^{ord}_{\theta_{BS}}(j,1)$, where $j = 1, y, \ldots$;
   If $\text{card}(\boldsymbol{b}_{\theta_{BS}}) \leq 3$ then $G = \boldsymbol{b}_{\theta_{BS}}$;
   If $\text{card}(\boldsymbol{b}_{\theta_{BS}}) > 3$ then the BS constructs $\boldsymbol{b}^{ord}_{\theta_{BS}}$ by ordering the angles in $\boldsymbol{b}_{\theta_{BS}}$ according to their percentage (descending) of presence in the *M-DB* points. BS selects $G = \boldsymbol{b}^{ord}_{\theta_{BS}}(1:3)$;
7. The BS illuminates the UE using all $\theta_{BS} \in G$. For each BS angle, the UE measures the power at $\theta_{UERUE} = \frac{(n-1)\pi}{6}$; $n = 1:1:12$ relative to the random initial angle θ_{UEinit}. The data set is saved as:

$$\boldsymbol{v}_q = \boldsymbol{v}_q(1:12,1) = [p_{q,1}, p_{q,2}, .., p_{q,12}]^T;$$
$$q = 1,2,3.$$

8. The UE applies interpolation and curve fitting to each extended vector:

$\left[\boldsymbol{v}_{qext}\right]_{24x1} = \left[\boldsymbol{v}_q(7:12,1); \boldsymbol{v}_q(1:12,1); \boldsymbol{v}_q(1:6,1)\right]$ to obtain $[\boldsymbol{v}''_{qext}]_{720x1}$; and then calculates
$[\boldsymbol{v}'_{qext}]_{360x1} = \boldsymbol{v}''_{qext}(181:540,1)$ and
$[V]_{360x3} = \left[\boldsymbol{v}'_{1ext}\boldsymbol{v}'_{2ext}\boldsymbol{v}'_{3ext}\right]$.

9. The UE determines $(\theta^b_{BS}, \theta^{1°}_{UEmaxPowRUE}) = (\underset{\theta_{BS},\theta_{UE}}{\operatorname{argmax}}\,\mathbf{V})$.
10. The UE maps $\theta^{1°}_{UEmaxPowRUE} \in [0°{:}1°{:}360°)$ to $\theta^{5°}_{UEmaxPowRUE} \in [0°:5°:360°)$
11. The UE feeds back the best angle θ^b_{BS}.
12. The BS applies θ^b_{BS}.
13. The UE changes to a narrower beamwidth antenna (horn 10°) and chooses the best θ^u_{UERUE} after measuring the power levels at: $\theta^{5°}_{UEmaxPowRUE} + (-10°, -5°, 0°, 5°, 10°)$.

The application of the best $\overline{N}$ BS angles instead of the total 121 possible ones in the step 2 of the Algorithm 2 reduces considerably the DB size.

The appropriate number of elements in the set G is determined by searching for the criteria that produce the performance closest to the maximum possible. The simulation results indicate the following:

- The selection (without any processing) of the BS angle that repeats the most inside å_{DB} does not offer a viable solution because the performance obtained (magenta-asterisk line in Figure 11) is considerably lower than the maximum possible (solid yellow). The selection of the two most probable BS angles inside å_{DB} (DB points) and the posterior application of the best of these two in terms of power delivery to the UE produces a performance (magenta dashed line) that is still not better than that of the modified hierarchical alignment method (dashed yellow line). A closer result (solid magenta line) to the maximum possible is obtained by selecting the three most frequent BS angles and the posterior application of the best of these three.
- The application of the BS angle $\boldsymbol{a}^{ord}_{\theta_{BS}}(1,1)$ results in a poor performance (blue asterisk, Fig. 11). The selection of the best of the BS angles $\boldsymbol{a}^{ord}_{\theta_{BS}}(1,1:3)$ (angles not separated in *bwdth*/2 degrees) in terms of power delivery to the UE produced a poor performance as well (green solid line).
- The selection of the best BS angle among $\boldsymbol{b}_{\theta_{BS}}(1,1:2)$ or $\boldsymbol{b}_{\theta_{BS}}(1,1:3)$ for the case of $n_a > 3$ (dashed or solid blue line, Fig. 11) produces a closer performance than those selected based on the probability criteria.
- The combination proposed in the algorithm 2 provides the closest performance (red) to the maximum possible.

Number of steps: Fewer steps are necessary in the application of proposed Algorithm 2 than in the modified classical hierarchical procedure because the BS directly applies a high-gain antenna at the beginning of the alignment task.

A simplified comparison is shown in Table 2. Only three additional UE power (angle) reads are sufficient in $\hat{a}_1$, reducing the total number of steps required to 24.

A more elaborate UE reading mechanism allows the use of only 4 instead of 5 additional power readings in $\hat{a}_2$.

The number of steps in Table 2 is the maximum possible for the proposed method. There are many cases in which the number of BS angles in G is less than 3.

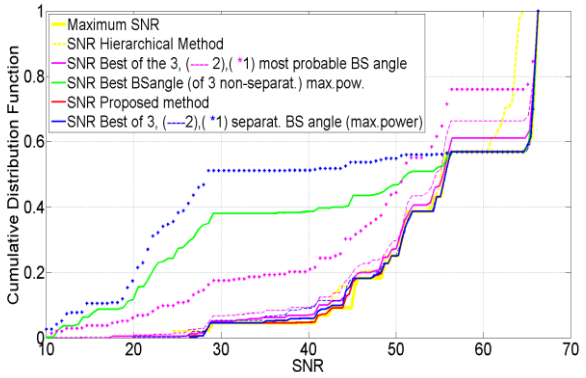

FIGURE 11. SNR at the UE using best BS angles selected based on power levels or repetition inside $\mathring{a}_{DB}$ ($\hat{a}_1$).

TABLE 2. Comparison of numbers of antenna alignment steps per 180° angle span.

BS H10°/H30° - UE H10°/H30°	Modified Hierarchical	Proposed method
UE determines best BS sector (30°)	24	18
UE feedbacks information to BS	4	3
UE checks power at θ_{UE} + [-10° -5° 0° 5° 10°]		5
UE determines best BS subsector (10°)	3	
UE feedbacks information to BS	1	
UE determines its best subsector (10°)	3	
UE determines best BS subsector θ_{BS} + [-2.5°	2	
UE feedbacks information to BS	1	
UE determines its best subsector θ_{UE} + [-2.5° 2.5°]	2	
Total (in 180°)	**40**	**26**

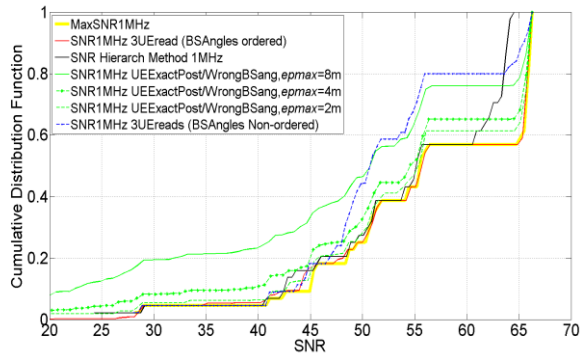

FIGURE 12. Performance of Algorithm 2 ($\hat{a}_1$); ***DBres*** = 0.5 m, D = 10 m, and e_{pmax} = 2 m, 4 m, and 8 m.

IV. ALGORITHM PERFORMANCE

A. STATIC CASE

Figures 12 and 13 show the performance of Algorithm 2 for $D = e_{pmax} = 10$ m and $DB_{res} = 0.5$ m. These results are achieved using three and five additional UE power readings for $\hat{a}_1$ and $\hat{a}_2$, respectively. The Figures also show (in green) the SNR at the UE for the case of the direct application of the best BS angle obtained from the DB using the inexact location reported by the UE for e_{pmax} of 2, 4 and 8m. The SNR difference relative to the maximum possible reaches 21 dB in $\hat{a}_1$ and 8 dB in $\hat{a}_2$ (it is actually higher for low SNR).

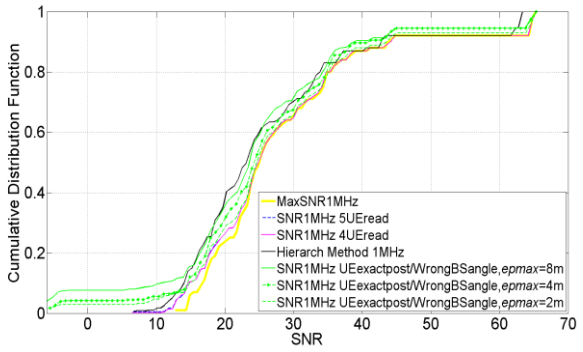

FIGURE 13. Performance of Algorithm 2 ($\hat{a}_2$); ***DBres*** = 0.5 m, D = 10 m, e_{pmax} = 2 m, 4 m, and 8 m.

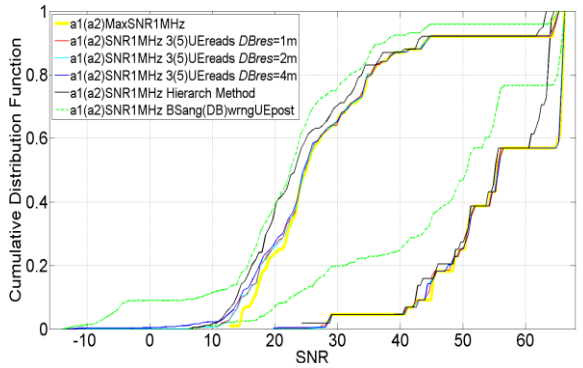

FIGURE 14. Performance of Algorithm 2 in $\hat{a}_1$ and $\hat{a}_2$. D = 10 m, DB_{res} = 1 m, 2 m, and 4 m.

An arbitrary selection of angles in $\boldsymbol{a}_{\theta_{BS}}$ (step 3 in Algorithm 2) results in a poor performance (dot-dashed blue line in Figure 12). The same simulation for $\hat{a}_2$ (Figure 13) is not shown because of the small impact in the received power. The selection of a larger number of BS angles (e.g., 4) in set G yields a very small improvement in performance but a large impact on the number of steps in the beam alignment. For each additional BS angle in set G, the number of power level measurements at the UE increases by 12.

Figure 14 shows the performance of Algorithm 2 for $e_{pmax} = D = 10$ m and different DB_{res} (1 m, 2m, and 4 m) for both areas. The repetition of the best BS angles in $\mathring{a}_{DB}$ helps maintain the performance with a small change when DB_{res} decreases. The performances are largely maintained without considerable variation for all the DB resolutions considered in $\hat{a}_1$ and up to 2 m in $\hat{a}_2$. In the latter case, a reverse situation begins to appear at approximately SNR = 10 dB for DB_{res} of 4 m (and 3 m; not shown). The figure also shows the SNR at the UE (solid green curves for both areas) when the BS applies an angle taken from the DB directly using the reported inexact location ($e_{pmax} = D = 10$m) for $DB_{res} = 4$m.

These results are interesting because they provide an opportunity to decrease the number of points needed for the DB. Specifically, for the current 60° × 200 m (20,944 m^2) sector, the number of DB points could be

decreased from 86,776 to 9,308 (5,249) if the resolution was decreased from 0.5 m to 1.5 m (2 m) with no considerable impact on performance.

B. RANDOM VARIATION OF THE MAXIMUM RECEIVED POWER

To evaluate the performance of Algorithm 2 for non-static conditions, we emulate a particular channel variation by replacing the PAP (function of the best θ_{BS} and θ_{UE}) at the UE with a new one corresponding to a DB point randomly located within a certain radius d_{DBr}, that is, $||X_{new} - X_{RP}||_2 \leq d_{DBr}$. This replacement can change the received maximum power and the best BS-UE angle combination.

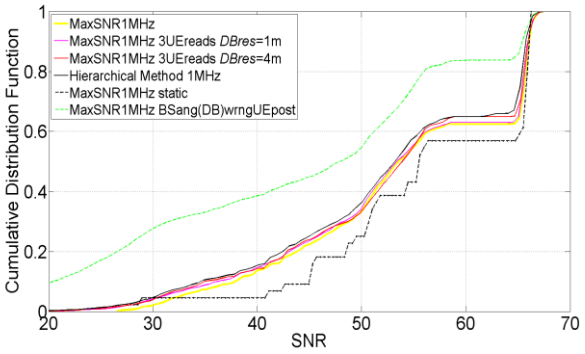

FIGURE 15. SNR comparison ($\hat{a}_1$); Variable power distribution at UE. DB_{res} = 1 and 4 m.

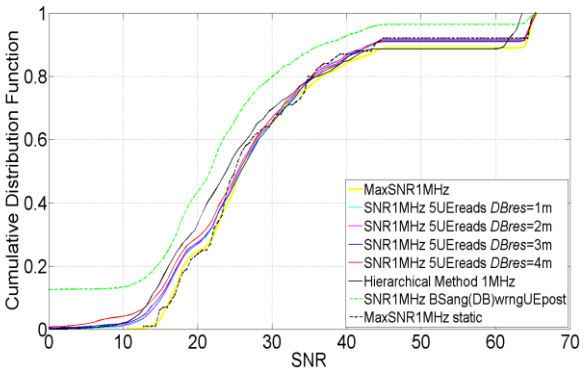

FIGURE 16. SNR comparison ($\hat{a}_2$); Variable power distribution at UE. DB_{res} = 1 m, 2 m, 3 m, and 4m.

Figures 15 and 16 show the performance for $D = e_{pmax} =$ 10m, $d_{DBr} = D$ and particular parameters of $DB_{res} = 1$ m, 4 m in $\hat{a}_1$ and $DB_{res} = 1, 2, 3$, and 4 m in $\hat{a}_2$. As expected, the actual maximum possible SNR (yellow line) has changed compared to the original one (dashed black line); the latter is linked to the best BS angle under static conditions. The power variation reaches a maximum value of approximately 10 dB in $\hat{a}_1$. The figures also show (green line) the maximum SNR in the case of the direct application of the best BS angle associated with inexact position information for $e_{pmax} = 10$ m and $DB_{res} = 4$ m (difference of 17 dB in $\hat{a}_1$ and 4.5 dB in $\hat{a}_2$ relative to the maximum possible). For DB_{res} up to 2 m, Algorithm 2 has a similar performance (excluding some locations in $\hat{a}_2$ where the SNR $\geq$ 35) as the modified classical hierarchical procedure in both $\hat{a}_1$ and $\hat{a}_2$ but uses fewer steps in the antenna alignment procedure (Table 2).

Simulations using $d_{DBr} > D$ are not considered. An external random event occurring near the UE that can cause a variation in the maximum received power changes the best UE and BS angles; the latter most likely changes to one that belongs to the group of angles best serving all M-DB points located in $\mathring{a}_{DB}$. The UE angle can change considerably; however, such changes do not impact the performance because the UE determines the best antenna orientation through a sequence of measurements.

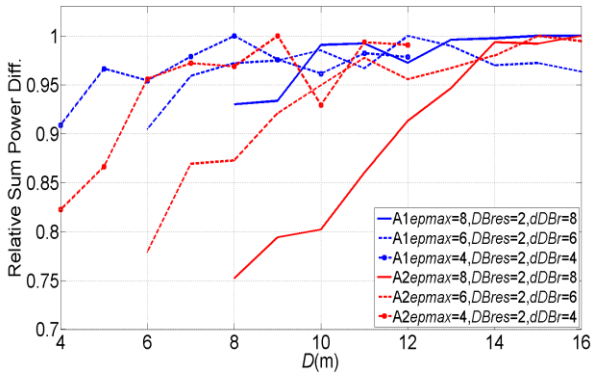

FIGURE 17. Relative Sum of the Power Difference versus D.

TABLE 3. D for first 'tspd" maximum value.

	e_{pmax}	$D(\hat{a}1)$	$D(\hat{a}1) > e_{pmax}$	$D(\hat{a}2)$	$D(\hat{a}2) > e_{pmax}$
DB_{res} 2m	8	11	38%	14	75%
	6	10	67%	11	83%
	4	5	25%	7	75%
	e_{pmax}	$D(\hat{a}1)$	$D(\hat{a}1) > e_{pmax}$	$D(\hat{a}2)$	$D(\hat{a}2) > e_{pmax}$
DB_{res} 1.5m	8	11	38%	15	88%
	6	10	67%	10	67%
	4	5	25%	7	75%

To determine whether the relation $D \gtrsim e_{pmax}$ is still valid when the power at a UE position varies, a simulation of the relative total sum of power differences ($tspd$) is performed in the form

$$tspd = \frac{ts}{\max(ts)}; \quad ts = \sum_{i=1}^{M} \left| P_{UEpi} - P_{UEHi} \right| \qquad (1)$$

where P_{UEpi} and P_{UEHi} represent the maximum power level measured by the UE$_i$ using Algorithm 2 and the modified classical hierarchical method, respectively, for $D = 6 : 1 : 16$; $e_{pmax} = d_{DBr} = 4$, 6, and 8 m, and $DB_{res} = 2(1.5)$ m for $\hat{a}_1$ and $\hat{a}_2$.

Figure 17 and Table 3 show that '$tspd$' in general increases up to a certain D, after which it varies with a minimum value higher than that corresponding to $D = e_{pmax}$. Moreover,

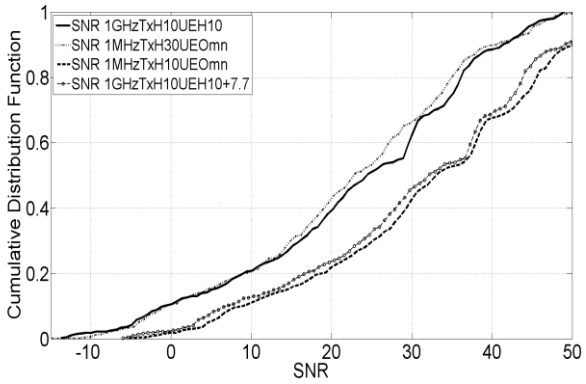

FIGURE 18. SNR comparison.

the variation is not sufficiently large to obtain a benefit by further increasing D. The factor '$max(ts)$' in (1) is inserted to accentuate the maximum '$tspd$' values. In all cases, the D value corresponding to the first maximum is larger than e_{pmax} at least in 25% for both areas $\hat{a}_1$ and $\hat{a}_2$ without a strong dependence on DB_{res}. Similar results were obtained for a DB_{res} of 1.5m. A total of 120 iterations are applied for each case.

The variation in the received power can be due to a sudden partial blocking or deviation (reflection) of the signal power emitted by the BS. The final impact on the performance depends on the difference in the power received by the UE using each angle in set G and the precision of the UE best angle determination obtained directly through the sequence of power measurements.

V. CONCLUSIONS

The results from ray tracing simulations in the 28 GHz band indicate that the use of a DB can become a resource for a faster antenna lock-on even in the case of non-exact knowledge of the position of a user. The current work proposes an algorithm that outperforms a modified classical hierarchical procedure in terms of the number of steps. This algorithm also provides the advantage of an initial larger power for antenna alignment. Such a result is obtained as long as the exact position is located inside the circular area of DB points (radius D) around the non-exact position reported by the UE. A practical setting for the D value depends on the average SNR in the area under study. In any case, such a value is larger than the accuracy of the positioning system at least in 25%. Specific-site simulations with different position errors up to 10 m and DB resolutions indicate that the DB point separation can be increased up to a distance of 2 m with no considerable impact on performance. This result relaxes the DB resolution requirements to a size that could be easily managed with current computation capabilities. The results exhibit consistency under random variations in the power levels at the UE.

APPENDIX

In contrast to a classical hierarchical procedure in the 60 GHz band, in which the beam alignment process starts in transmit or receive mode with one of the sides using an omnidirectional antenna, its direct implementation in the 28 GHz band becomes problematic. The large propagation path loss cannot be fully compensated with such antenna gains. This effect can be observed by considering the maximum SNR_o ($=SNR_{1GHzTH10UEH10}$) obtained in a system (Figure 1) comprising a BS serving 500 arbitrary positions of a user. The BS and UE are equipped with (3-dB beamwidth) 10° horn antennas and operate with a bandwidth of 1 GHz. For this task, we let the BS use the best angles found in the range [−60°:1°:60°], whereas the UE angle varies in [0°:5°:355°]. Figure 18 shows (solid black) that a certain percentage of users cannot reach a defined target SNR (e.g., 2 dB) to comply with a minimum rate.

A lower signal bandwidth can be used to have any UE connected using smaller antenna gains, as applied in a classical hierarchical antenna alignment method. Table 4 shows the quantity in dB that must be added in the approximate calculation of a different $SNR_{New} = SNR_o - (G_{Txo} + G_{Rxo}) + (G_{TxNew} + G_{RNew}) + G_F$. G_{Txo}, $G_{Rxo}(G_{TxNew}, G_{RxNew})$ represent the Tx and Rx antenna gains used in the calculation of the reference SNR_o (SNR_{New}), respectively, and G_F is the gain caused by a change in the bandwidth. The last 2 lines correspond to setups in which the BS and UE are equipped with planar arrays.

TABLE 4. SNR compensation.

$G_{TH10} = 24.45$ dB, $G_{TH30} = 15$ dB, $G_{Omn(dipole)} = 2.15$ dB, $G_F = 30$ dB			
$SNR_{1MHzTH30UEOmn}$	$= SNR_{1GHzTH10UEH10}$	-	1.75
$SNR_{1MHzTH10UEOmn}$		+	7.70
$SNR_{1MHzTH30UEH30}$		+	11.10
$SNR_{1MHzTH10UEH30}$		+	20.55
$SNR_{1MHzTA2x8UEA2x4}$		+	1.17
$SNR_{1MHzTA2x10UEA2x10}$		+	6.12

Applying the relation $R = \beta \Delta W \log_2(1 + \text{SNR})$ [22], where $\beta = (0.5)(0.8)$ for half-TDD constraints and 20% control overhead, $\Delta W = 1$ MHz and a signal duration of 100 μs, the minimum SNR required for a target rate of 100 kbps corresponds to −4.73 dB. In other words, at least 8 dB of additional power is required at some locations to ensure that all the UEs have access connection viability within the service area.

The configuration 1MHzTH30UEOmn cannot provide this gain. Alternatively, the configurations 1MHzTH30UEH30, 1MHzTH30UEH10 and 1MHzTxH10UEH10 provide more than the required gain. Table 4 also shows that the application of an array of 2 antenna elements for the azimuth beam steering (beamwidth of 52.9°) that could lower the number of steps in a hierarchical alignment procedure would not facilitate the initial link possibility at some locations. Wide

uniform beams can be designed for channel estimation using hybrid beamforming, but a larger number of RF fronts are needed [10].

REFERENCES

[1] S. Rangan, T. S. Rappaport, and E. Erkip, "Millimeter wave cellular wireless networks: Potentials and challenges," *Proc. IEEE*, vol. 102, no. 3, pp. 366–385, Mar. 2014.
[2] *Part 15.3: Wireless Medium Access Control (MAC) and Physical Layer (PHY) Specifications for High Rate Wireless Personal Area Networks (WPANs)*, IEEE Standard 802.15.3c, 2009.
[3] E. Perahia, C. Cordeiro, M. Park, and L. L. Yang, "IEEE 802.11ad: Defining the next generation multi-Gbps Wi-Fi," in *Proc. IEEE CCNC*, Las Vegas, NV, USA, 2010, pp. 634–638.
[4] J. Wang *et al.*, "Beam codebook based beamforming protocol for multi-Gbps millimeter-wave WPAN systems," *IEEE J. Sel. Areas Commun.*, vol. 27, no. 8, pp. 1390–1399, Oct. 2009.
[5] S. Hur, T. Kim, D. J. Love, J. V. Krogmeier, T. A. Thomas, and A. Ghosh, "Millimeter wave beamforming for wireless backhaul and access in small cell networks," *IEEE Trans. Commun.*, vol. 61, no. 10, pp. 4391–4403, Oct. 2013.
[6] Q. C. Li, H. Niu, G. Wu, and R. Q. Hu, "Anchor-booster based heterogeneous networks with mmWave capable booster cells," in *Proc. IEEE Globecom Workshops (GC Wkshps)*, Dec. 2013, pp. 93–98.
[7] A. Alkhateeb, G. Leus, and R. W. Heath Jr., "Compressed sensing based multi-user millimeter wave systems: How many measurements are needed?" in *Proc. IEEE Int. Conf. Acoust., Speech Signal Process. (ICASSP)*, Aug. 2015, pp. 2909–2913.
[8] D. E. Berraki, S. M. D. Armour, and A. R. Nix, "Application of compressive sensing in sparse spatial channel recovery for beamforming in mmWave outdoor systems," in *Proc. IEEE Wireless Commun. Netw. Conf. (WCNC)*, vol. 1. Apr. 2014, pp. 887–892.
[9] O. El Ayach, S. Rajagopal, S. Abu-Surra, Z. Pi, and R. W. Heath, Jr., "Spatially sparse precoding in millimeter wave MIMO systems," *IEEE Trans. Wireless Commun.*, vol. 13, no. 3, pp. 1499–1513, Mar. 2013.
[10] A. Alkhateeb, O. El Ayach, G. Leus, and R. W. Heath, Jr., "Channel estimation and hybrid precoding for millimeter wave cellular systems," *IEEE J. Sel. Topics Signal Process.*, vol. 8, no. 5, pp. 831–846, Oct. 2014.
[11] S. Sand, R. Tanbourgi, C. Mensing, and R. Raulefs, "Position aware adaptive communication systems," in *Proc. Conf. Rec. 43rd Asilomar Conf. Signals, Syst. Comput.*, 2009, pp. 73–77.
[12] R. Di Taranto, S. Muppirisetty, R. Raulefs, D. Slock, T. Svensson, and H. Wymeersch, "Location-aware communications for 5G networks: How location information can improve scalability, latency, and robustness of 5G," *IEEE Signal Process. Mag.*, vol. 31, no. 6, pp. 102–112, Nov. 2014.
[13] A. Capone, I. Filippini, and V. Sciancalepore. (2015). "Context-based cell search in millimeter wave 5G networks." [Online]. Available: https://arxiv.org/abs/1501.02223
[14] A. Capone, I. Filippini, V. Sciancalepore, and D. Tremolada, "Obstacle avoidance cell discovery using mm-waves directive antennas in 5G networks," in *Proc. IEEE Int. Symp. Pers., Indoor Mobile Radio Commun. (PIMRC)*, Dec. 2015, pp. 2349–2353.
[15] V. Degli-Esposti *et al.*, "Ray-Tracing-Based mm-Wave Beamforming Assessment," *IEEE Access*, vol. 2, pp. 1314–1325, 2014.
[16] W. Abbas and M. Zorzi. (May 2016). "Context information based initial cell search for millimeter wave 5G cellular networks." [Online]. Available: https://arxiv.org/abs/1605.01930
[17] S. Ferrante, T. Deng, R. Pragada, and D. Cohen, "mm wave initial cell search analysis under UE rotational motion," in *Proc. IEEE Int. Conf. Ubiquitous Wireless Broadband*, 2015, pp. 1–7.
[18] J. C. Aviles and A. Kouki, "Exploiting site-specific propagation characteristics in directional search at 28 GHz," *IEEE Access*, vol. 4, pp. 3894–3906, 2016.
[19] RemCom. (2016). *Wireless InSite*. [Online]. Available: http://www.remcom.com/wireless-insite
[20] C. A. Balanis, *Antenna Theory: Analysis and Design*, 3rd ed. Hoboken, NJ, USA: Wiley, 2005.
[21] L. Harry and V. Trees, *Optimum Array Processing: Part IV of Detection, Estimation, and Modulation Theory*. New York, NY, USA: Wiley, 2002.
[22] C. Barati, S. Hosseini, S. Rangan, P. Liu, T. Korakis, and S. Panwar, "Directional cell search for millimeter wave cellular systems," in *Proc. IEEE 15th Int. Workshop Signal Process. Adv. Wireless Commun.*, Toronto, ON, Canada, Apr. 2014, pp. 120–124.

JUAN C. AVILES (M'10) received an Electrical Engineering degree from Escuela Superior Politécnica del Litoral (ESPOL) in 1982 and an M.S. degree in Electrical Engineering from Syracuse University in 1986. He is currently a Ph.D. student at the École de technologie supérieure, Montreal, QC, Canada. He has been a Professor at the Faculty of Electrical and Computer Engineering, ESPOL, and an Advisor in the radio communications field. His research interests are propagation and intelligent antenna applications for mobile systems in mmW bands.

AMMAR KOUKI (S'88–M'92–SM'01) received the B.S. (Hons.) and M.S. degrees in engineering science from Pennsylvania State University in 1985 and 1987, respectively, and the Ph.D. degree in electrical engineering from the University of Illinois at Urbana–Champaign in 1991. He is currently a Full Professor of Electrical Engineering and the Founding Director of the LTCC@ETS Laboratory with the École de technologie supérieure, Montreal, QC, Canada. His research interests are in the areas of active and passive microwave and mm-wave devices and circuits, intelligent and efficient RF front-ends, 3-D circuits in LTCC, applied computational electromagnetics, and antennas radio-wave propagation modeling.